Kinetics of the Cyclopentadiene Decay and the Recombination of Cyclopentadienyl Radicals with H-Atoms: Enthalpy of Formation of the Cyclopentadienyl Radical

K. ROY, M. BRAUN-UNKHOFF, P. FRANK, TH. JUST

DLR *Institut für Verbrennungstechnik, Bergstrasse, Frankendof,* 96155 *Buttenheim, Stuttgart, Germany*

Received 12 June 2001; accepted 23 August 2001

ABSTRACT: The recombination of c-C_5H_5 with H-atoms has been studied behind reflected shock waves. The obtained rate coefficients are almost independent of temperature and were found to be $k_{\mathrm{rec}} = 2.6 \times 10^{14}$ cm^3 mol^{-1} s^{-1} for pressures around 2 bar in the temperature range between 1150 and 1500 K. Together with rate coefficients for the dissociation, obtained in an earlier work (Roy et al., Proc Combust Inst 1998, 27, 329–336) at pressures and temperatures close to those applied in the present work, we calculated equilibrium constants $K_c(T)$ for $C_5H_6 \rightleftharpoons$ c-$C_5H_5 + H$. A "third law" analysis was performed. Data for the enthalpy of formation of cyclopentadienyl $DH_{f,0} = 65.4 \pm 1$ kcal mol^{-1} and $DH_{f,298} = 62.5 \pm 1$ kcal mol^{-1} were derived, respectively. The analysis was based upon new results on the entropy of cyclopentadienyl, recently calculated by Kiefer et al. (J phy chem, in press). Finally, our measured data were subjected to a fall-off analysis. The simulation turned out very satisfactorily. © 2001 John Wiley & Sons, Inc. Int J Chem Kinet 33: 821–833, 2001

INTRODUCTION

Quantitative modeling of soot formation in flames requires rather detailed chemistry models. In the last decade it became more and more apparent that exact kinetic data for the benzene/phenyl subsystem play a key role in the complex chemistry of soot production as well as of the soot reduction. Phenyl reactions with molecular oxygen lead to phenoxy and in a further fast decay of phenoxy to cyclopentadienyl radicals and CO [1]. Phenol, which is an intermediate appearing on the route of benzene oxidation, can also be easily converted

---

Correspondence to: Th. Just; e-mail: thomas.just@t-on-line.de.

to cyclopentadiene and CO. This happens very likely through a keto-enol tautomerization at elevated temperatures [2]. According to theoretical work [3] there might exist a route leading by the association of two cyclopentadienyl radicals to either naphthalene or to naphthyl radicals +H-atoms. This route, if existing, can, under certain fuel-to-oxygen ratios in a flame, contribute to the formation of PAHs. Experimental data on the formation of cyclopentadiene as an intermediate in a flame exist [4]; however, a simulation of measured concentration profiles has not been very successfull up to now (see e.g. [5,6]). The role of the five-membered rings in the complex reaction system, typical for a sooting flame, is not fully understood presently.

In an earlier study, we performed measurements of the dissociation of cyclopentadiene to $c\text{-}C_5H_5 + H$ [7]. In the present work, we focus our interest on the cyclopentadienyl radical and report here on an experimental investigation on the reverse reaction. To our knowledge there are no experimental studies yet on the recombination reaction $c\text{-}C_5H_5 + H$. But there exist theoretical calculation studies on the reaction mechanism of the $c\text{-}C_5H_5$ radical, e.g. by Dean [8a] and Zhong and Bozzelli [8b]. For the benzene and toluene oxidation mechanism, Emdee et al. [9] estimated a temperature independent value for $c\text{-}C_5H_5 + H$. The rate coefficients given in the aforementioned studies are listed in Table I. The coefficient determined by Dean is valid for 1038 K and the one by Zhong and Bozzelli for 1100 K (the same temperature as in the experiment of Lovell et al. [10]). Still, in the work of Zhong et al. a discrepancy of about a factor 2 is found between the calculated and measured concentrations of cyclopentadiene.

To properly interpret experimental flame data it is absolutely necessary to use the most precise thermodynamic data available for kinetic calculations. Presently, there exist larger uncertainties inherent in the published thermodynamic data. This refers to the enthalpy of formation as well as to the entropy of $c\text{-}C_5H_5$ [11–13]. From our two sets of rate coefficients, obtained almost in the same temperature and pressure range, we calculated the equilibrium constants and derived from these the reaction enthalpy. Our computations profited greatly on new, unpublished entropy data stemming from Kiefer et al. [14]. A fall-off analysis of our data is also presented.

Table I Published Data on $c\text{-}C_5H_5 + H \rightarrow C_5H_6$

k	T	Reference
5.96×10^{13}	1038	[8a]
3.2×10^{14}	1100	[8b]
1.0×10^{14}	^{a}	[9]

Units are cm^3, s, mol, K.

^{a}No T-range given.

EXPERIMENTAL

The thermal decomposition of cyclopentadiene and the recombination of the cyclopentadienyl radical with H-atoms

$$C_5H_6 \rightarrow c\text{-}C_5H_5 + H \qquad (R1)$$

$$c\text{-}C_5H_5 + H \rightarrow C_5H_6 \qquad (R\text{-}1)$$

were studied behind reflected shock waves.

The high purity, heatable stainless steel shock tube used in this study consists of a test section of 6 m and a driver section of 4 m in length. The internal diameter is 7.2 cm. The test section is evacuated to about 10^{-7} mbar before each experiment by a turbomolecular pump. A detailed description of the apparatus is given elsewhere [15].

Atomic resonance absorption spectroscopy (ARAS) was used to monitor the temporal concentration profiles of hydrogen- and iodine-atoms. The H-atom absorption was measured at a wavelength $\lambda = 121.6$ nm by using an oxygen spectral filter, the I-atom absorption at $\lambda = 164.2$ nm using a monochromator. The concentration profiles of H-atoms reported here are based on calibration experiments using the reaction of O-atoms with H_2 to produce H-atoms [15]. In the case of I-atoms, the dissociation of methyliodide was used for calibration [16].

The ARAS technique allows high temperature reactions to be studied in highly diluted mixtures where temperature effects caused by the ongoing of the reactions are of no importance. Further, these low initial concentrations strongly reduce, within the time scale of the experiment ($t \leq 800\ \mu s$), the number of subsequent reactions that had to be considered for the evaluation of the measured concentration profiles.

$C_5H_6 \rightarrow C_5H_5 +$ H Dissociation Reaction

The C_5H_6 decomposition was studied for mixtures of 0.5 up to 10 ppm at temperatures between 1200 and 1600 K and pressures between 1 and 5 bar [7]. Cyclopentadiene was obtained by distillation from dicyclopentadiene with a purity of better than 99% (controlled by mass spectrometry). The initial concentrations of cyclopentadiene were routinely measured in samples drawn from the shock tube. The probes were analyzed by a gas-chromatograph coupled to a flame ionization detector. The detection limit was about 0.5 ppm at 100 mbar total pressure. The diluent in all experiments was highly purified Argon (Ar = 99.9999%).

Quite recently, Backsay and Mackie [17] published theoretical calculations on the possible decay channels of C_5H_6. Additionally to the simple C—H bond fission of the cyclopentadiene they found molecular channels leading, via hydrogen shifts followed by a C—C fission, eventually to chain molecules. The lowest barrier was found for $CH_2CHCHCCH_2$, whereby the calculated barrier height is on the order of the C—H bond fission for cyclopentadiene. The formed $CH_2CHCHCCH_2$ molecule then decomposes by a further C—C fission into C_2H_2 and methylacetylene. We performed some model calculations introducing the additional channels. Within our experimental temperature range a practically negligible effect on the H-atom profiles for $[C_5H_5]_0 \leq 10$ ppm was observed.

c-C_5H_5 + H Recombination Reaction

The experiments were conducted with concentrations of 0.5–1.2 ppm for $[C_5H_5]_0$ and 0.2–2.5 ppm for $[H]_0$. Experimental temperatures ranged from 1100 to 1600 K at total pressures of about 2 bar. For measuring the recombination of the cyclopentadienyl radical with H-atoms, cyclopentadienyliodide (C_5H_5I) served as a thermal source for the cyclopentadienyl radical. H-atoms were produced by the thermal decay of ethyliodide (C_2H_5I).

The initial concentration of C_5H_5I was determined by measuring the atomic resonance absorption of Iodine atoms and calculating the concentration from calibration experiments. The decomposition of C_5H_5I was studied in a separate series of experiments [18]. It was found that above 780 K, C_5H_5I dissociates completely into the cyclopentadienyl radical and an Iodine-atom within only 30 μs. Therefore, the derived I-atom concentration yields directly the initial c-C_5H_5 concentration. The I-atom concentration was correlated to measurements of c-C_5H_5I by gas chromatography.

Mixtures with varying ratios of C_2H_5I and C_5H_5I were prepared. For each experiment the H-and I-atom-absorptions were simultaneously detected. The initial H-atom concentration was then determined from extrapolation of the H-absorption signal to $t = 0\,\mu$s. It was shown that ethyliodide yields one H-atom for each I-atom, that splits off the molecule [19]. The I-ARAS signal gives the absorption of I-atoms from both the dissociation reactions of C_5H_5I and of C_2H_5I. The concentration of C_5H_5I was then derived from the measured I-absorption. The error in the concentration is about 20% for the range $[C_5H_5]_0 \leq$ 1 ppm.

RESULTS

c-C_5H_5 + H Recombination Reaction

Figure 1 shows an experimental concentration profile of H-atoms, measured during the reaction of c-C_5H_5 with H-atoms. In this figure, the simulation of the measured H profile using the small reaction scheme given in Table II is demonstrated, in particular with respect to the rate coefficient k_{rec}.

For modeling two possible reaction channels for the reaction of c-C_5H_5 radicals with H atoms were considered:

$$\text{c-}C_5H_5 + H \rightarrow C_5H_6 \qquad \text{(R-1)}$$

$$\text{c-}C_5H_5 + H \rightarrow C_5H_4(^1A_1) + H_2 \qquad \text{(R-1a)}$$

Wang and Brezinsky [12] calculated a value for the endothermicity of 16 kcal mol^{-1} for channel R-1a. This value was used in the present work for modeling, assuming no additional barrier for this reaction. We follow the arguments as outlined in [12] for this reaction. Further, the corresponding A-factor was varied between 10^{14} and 10^{16} cm^3 mol^{-1} s^{-1}. Even with this high A-factor, which is above the upper limit for a rapid abstraction reaction, no influence on the H-profiles was found. Additionally, no temperature dependence was detected in the experimental data, which led us to the assumption that $k_{-1a}/k_{-1} < 0.01$. Therefore, R-1a can be safely neglected for our experimental conditions. Figure 1 shows a strong influence on the H-disappearance if the rate coefficient for R-1 is varied by ±50%. Thus, a rate coefficient can be easily derived from the simulation of each of the recorded

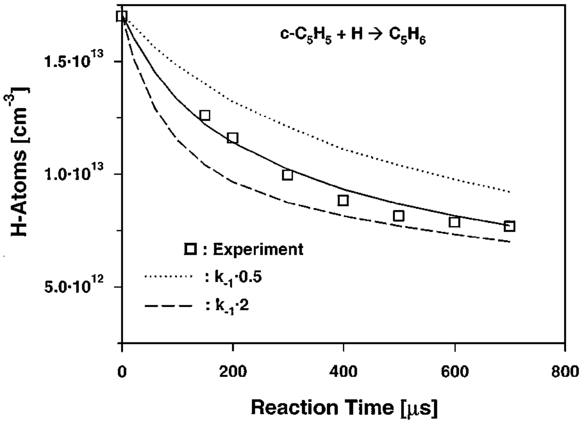

Figure 1 Modeling of the H-concentration and sensitivity on the rate coefficient for the reaction R-1 c-C_5H_5 + H → C_5H_6; experimental conditions: $T = 1198$ K, $p = 2.0$ bar, $[C_5H_5]_0 = 0.7$ ppm, $[H]_0 = 1.5$ ppm (diluted with Ar).

Table II Reaction Mechanism Used for Modeling the Measured H Atom Profiles of the Reaction R-1: c-$C_5H_5 + H \rightarrow C_5H_6$

Reaction no.	Reaction	*A*	*n*	E_a/R	Reference
R-1	c-$C_5H_5 + H \rightarrow C_5H_6$	2.6×10^{14}	0	0	Present work
R2	$C_5H_6 + H \rightarrow$ c-$C_5H_5 + H_2$	2.8×10^{13}	0	1137	[9] [20]
R1	$C_5H_6 \rightarrow$ c-$C_5H_5 + H$	4.0×10^{14}	0	38760	[2]
R3	2 c-$C_5H_5 \rightarrow C_{10}H_8 + 2H$	2.0×10^{13}	0	2010	[21]

Units are cm^3, s, mol, K.

H-absorption profiles to be

$$k_{-1} = 2.6 \times 10^{14}\ \mathrm{cm^3\ mole^{-1}\ s^{-1}}$$
$$\text{for } T = 1100\text{–}1400\ \mathrm{K} \text{ at } p_{\mathrm{tot}} \approx 2\ \mathrm{bar}$$

The error in the rate coefficient is mainly caused by the determination of the initial c-C_5H_5 concentration, which was described above. The resulting scatter is of the order of ±25%. The profiles could be simulated with the small set of reactions listed in Table II. The self-combination R3, i.e. 2c-$C_5H_5 \rightarrow C_{10}H_8 + 2H$, becomes important only for ratios [c-$C_5H_5]_0/[H]_0 \geq 3/1$, when cyclopentadienyl is present in higher amounts.

Data Evaluation, Equilibrium Constant for $C_5H_6 \rightleftharpoons$ c-$C_5H_5 + H$

From the two sets of measurements, decay of C_5H_6 and recombination of c-$C_5H_5 + H \rightarrow C_5H_6$, the respective rate coefficients were used to calculate the equilibrium constants in the temperature range from 1100 to 1600 K. The rate coefficient k_{diss} was determined between 1200 and 1600 K (see Roy et al. [7]), and the recombination coefficient k_{rec} between 1100 and 1450 K [22]. The data of k_{diss} at pressures around 2 bar were subjected to a first-order regression analysis. The corresponding Arrhenius expression (see Fig. 2) is

$$k = 1.7 \times 10^{14} \exp(-37530/T)\ \mathrm{s^{-1}}$$
$$1200 \leq T \leq 1600\,\mathrm{K}$$

First, we assumed that $k_{\mathrm{rec}} = 2.6 \times 10^{14}\ \mathrm{cm^3\ mol^{-1}\ s^{-1}}$ could be linearly extrapolated to the upper limit of 1600 K of our experiments on dissociation (see Fig. 3). In a second approximation, based upon a fall-off analysis, we interpolated k_{rec} by a regression function of second order, taking a weak temperature dependence into account (see discussion later).

The equilibrium constant $K_{\mathrm{c,exp}}(T)$, defined as $k_{\mathrm{diss}}/k_{\mathrm{rec}}$, is represented in the case of k_{rec} = constant by

$$K_{\mathrm{c,exp}}(T) = 0.653 \exp(-37530/T)\ \mathrm{mol\ cm^{-3}}$$

By a so called third-law analysis, $K_{\mathrm{c,exp}}(T)$ has to be compared with the appropriate expression of statistical thermodynamics:

$$K_{\mathrm{c}}(T) = \frac{Q_{\mathrm{c\text{-}C_5H_5}} Q_{\mathrm{H}}}{Q_{\mathrm{C_5H_6}}} \exp\left(-\frac{\mathrm{D}H_{\mathrm{r,0}}}{RT}\right)$$

The Q_i are the partition functions for the respective molecules given in mol $\mathrm{cm^{-3}}$. Provided the molecular parameters are sufficiently well known, Q_i can be easily calculated. Comparison of $K_{\mathrm{c}}(T)$ over the given T-range with $K_{\mathrm{c,exp}}(T)$ allows then to determine the enthalpy of reaction $\mathrm{D}H_{\mathrm{r,0}}$ and eventually the enthalpy of formation $\mathrm{D}H_{\mathrm{f,0}}$ for cyclopentadienyl. For Q_{H} and $Q_{\mathrm{C_5H_6}}$ the molecular data from Burcat's tables [23] were used. A complete set of experimental molecular data for c-C_5H_5 is not available, in particular the experimental data for the vibration frequencies are incomplete (see e.g. the few data given in

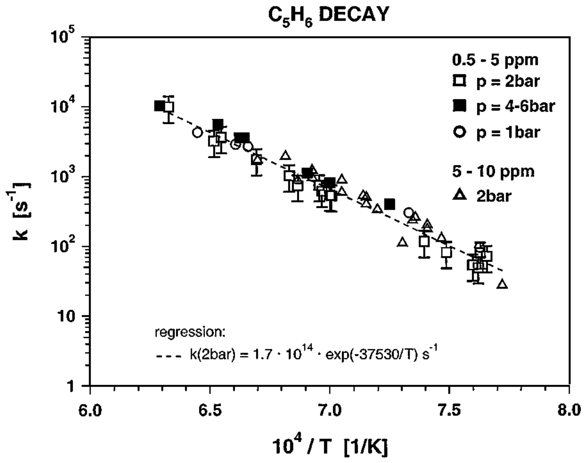

Figure 2 Decay of C_5H_6. Rate coefficients for the reaction R1 $C_5H_6 \rightarrow$ c-$C_5H_5 + H$ obtained in the pressure range from 1 to 6 bar [7].

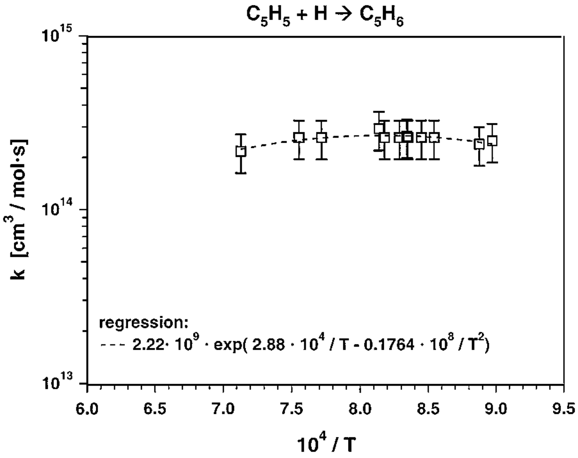

Figure 3 Rate coefficients for the recombination of c-C_5H_5 with H. $p \approx 2$ bar.

Table III Molecular Parameters

Frequencies (cm^{-1}) and used degeneracy	
c-C_5H_5[a]	C_5H_6[b]
3104 (1)	3105 (1)
3089 (2)	3091 (1)
3072 (2)	3075 (1)
1396 (2)	3043 (1)
1271 (1)	2900 (1)
1146 (2)	2886 (1)
1086 (1)	1580 (1)
990 (2)	1500 (1)
874 (2)	1378 (1)
874 (2)	1365 (1)
793 (2)	1292 (1)
746 (2)	1239 (1)
635 (1)	1100 (1)
505 (2)	1106 (1)
	1090 (1)
	994 (1)
	959 (1)
	941 (1)
	925 (1)
	915 (1)
	891 (1)
	805 (1)
	802 (1)
	700 (1)
	664 (1)
	516 (1)
	350 (1)

[a] Electronic degeneracies: $g_{el} = 2$ (see text); Rotational constants (cm^{-1}): $A = 0.295$; $B = 0.295$; $C = 0.147$; Symmetry factor = 10. *Source*: Kiefer et al. [14]. The two vibrations associated with the valence isomerisation were semiempirically modeled. The harmonic vibration was taken as 1542 cm^{-1} and the anharmonic energy levels as $E_{viso} = 600\ \upsilon_{iso}{}^2$ (see text).

[b] Electronic degeneracies: $g_{el} = 1$. Rotational constants (cm^{-1}): $A = 0.298$; $B = 0.275$; $C = 0.147$; Symmetry factor = 2. Parameters for Z_{LJ}; $\sigma_{AR} = 3.76$ Å; $\sigma_{C_5H_6} = 5.2$ Å; $(\varepsilon/k)_{AR} = 143$ K; $(\varepsilon/k)_{C_5H_6} = 400$ K; $\sigma_{KR} = 4.01$ Å; $(\varepsilon/k)_{KR} = 201$ K. Source: Castelucci et al. [24].

the NIST Chemistry-Webbook (http//webbook.nist.gov/chemistry)). Therefore, in case of the cyclopentadienyl radical we rely upon theoretical calculations performed, e.g., by Wang and Brezinsky [12], by Moskaleva and Lin [13], and quite recently by Kiefer et al. [14]. The set of molecular parameters used in our calculations is given in Table III.

The special problem regarding the cyclopentadienyl radical is its predicted facile change in space of its basic C_{2v} structure (valence isomerization see e.g. [25]). This is caused by the Jahn–Teller effect [26]. Recent quantum chemical calculations by Wang and Brezinsky [12] as well as by Moskaleva and Lin [13] have revealed that for this valence isomerization the pertinent barrier is almost negligible. This conclusion agrees with earlier calculations by Günthard and his coworkers [25b]. In both the recent investigations [12,13], it was proposed to model the valence isomerization by assuming a pseudo free rotor. Both groups ascribed a moment of inertia to this "pseudo free rotor" being equal to that belonging to the axis perpendicular to the molecular plane. The contribution of such a "free rotor" to the entropy is rather high. There is in our opinion no physical basis for a model of this type. In the most recent work of Kiefer et al. [14], the entropy problem was treated by means of a very high level quantum chemical calculation. The Jahn–Teller distortion potential was determined and a full set of energy levels for the nuclear motions on this potential was calculated. The entropy of cyclopentadienyl in the range from 300 to 2000 K is reproduced from this work in Table IV. We need for our modeling, equilibrium coefficients in the temperature range from about 1000 K up to 2500 K. In particular, data at the highest temperature have to be used in order to compare the experimental data on the C_5H_5 decay obtained by Kern et al. [11] with our fall-off analysis. There are two choices to proceed. Either we could extrapolate $K_c(T)$ data obtainable from the results on $H(T)$-$H(298)$ and $S(T)$ of [14] given for the restricted T-range 300–2000 K, or we could try to model the partition functions for C_5H_5 by a semiempirical method. We decided to do the latter, since a simple extrapolation of $K_c(T)$ from 2000–2500 K might cause larger errors which cannot be quantified. For our purpose, we assumed a harmonic/anharmonic oscillator model adapted to the results obtained with the full analysis (see e.g. [14]). The Jahn–Teller effect distorts the symmetric E_2' in-plane stretch and bending vibrations of the C_5-skeleton, starting with the D_{5h} symmetry. The resulting distortion is strong only for

Table IV Entropies of c-C_5H_5 as a Function of Temperature

T/K	S^0 (cal mol^{-1} K^{-1})
300	63.507
400	70.083
500	76.270
600	81.834
700	86.947
800	91.717
900	96.204
1000	100.44
1100	104.45
1200	108.25
1300	111.86
1400	115.29
1500	118.56
1600	121.68
1700	124.65
1800	127.50
1900	130.22
2000	132.83

The Jahn–Teller distortion was fully taken into account by a high level quantum chemical computation performed by A. Wagner and his group. For details see Kiefer et al. [14].

the two in-plane stretch motions [14,25(b)] and may be approximately described by a set of one harmonic vibration with 1542 cm^{-1} and an anharmonic oscillator with semiempircally modeled energy levels as $E_{\text{viso}} = D_{\text{viso}}\nu_{\text{iso}}^2$ [cm^{-1}] (see also [14]). By comparing our entropy data with that given in [14], we determined the parameter D_{viso} to $D_{\text{viso}} \approx 600$ cm^{-1}. The other vibrational (scaled) frequencies were taken from [14] obtained for the C_5H_5 (D_{5h} structure) (Table III). The electronic degeneracy is given by the electron spin and is 2. The calculated Jahn–Teller energy levels as given in [14] are composed of contributions of the two low electronic states: $^2B_1$ and $^2A_2$. Thus, the orbital degeneracy is inherently present in these calculations. The entropies calculated by us, using the partition function of cyclopentadienyl agree within less than 0.4% with the data of Kiefer et al. [14] in the temperature range from 600 to 2000 K. Almost the same is true for our calculation of the sensible heat $H(T)$-$H(298)$. These data agree within less than 1%.

With the molecular data for the cyclopentadienyl radical theoretically obtained, we calculated the temperature dependent preexponential factor $A_c(T)$ of $K_c(T)$:

$$K_c(T) = \frac{Q_{\text{c-}C_5H_5}\, Q_H}{Q_{C_5H_6}} \exp\left(-\frac{DH_{r,0}}{RT}\right) = A_c(T)\exp\left(-\frac{DH_{r,0}}{RT}\right)$$

$$A_c(T) = 1.533 \times 10^5\, T^{-1.1833} \exp(-1813/T) \text{ mol cm}^{-3} \quad 700 \le T \le 2500\ K$$

Comparing $K_{c,\exp}(T)$ as given above with $K_c(T)$ we obtain for three selected temperatures the following $DH_{r,0}$ values for the reaction set $C_5H_6 \rightleftharpoons \text{c-}C_5H_5 + H$: 1200 K: $DH_{r,0} = 80.3$ kcal mol^{-1}; 1400 K: $DH_{r,0} = 81.4$ kcal mol^{-1}; 1600 K: $DH_{r,0} = 82.4$ kcal mol^{-1}. The arithmetic mean is $DH_{r,0} = 81.37$ kcal mol^{-1}. Provided that the molecular parameters used in our calculation are sufficiently accurate, the slight increase in $DH_{r,0}$ with temperature likely reflects the combined experimental inaccuracies of our measurements.

However, some improvement of the data evaluation seems possible. Selecting experimental data obtained at about 2 bar, it is to be expected that in our experimental temperature range fall-off effects will be present. The scatter of the data for the rate coefficients of the dissociation is rather large. So it was decided to apply to the 2 bar data a first-order regression analysis only. On the other hand, the scatter of the data of the recombination experiments is considerably smaller. The trend of these data with increasing temperature seems to point to the presence of some fall-off effect in the investigated temperature range. Thus, application of a second-order regression analysis to the recombination coefficients may provide some improvement. We arrived at the representation:

$$k_{\text{rec}} = 2.22 \times 10^9 \exp(2.880 \times 10^4/T - 0.1764 \times 10^8/T^2)\,\text{cm}^3\,\text{mol}^{-1}\,\text{s}^{-1}$$

The regression analysis showed, perhaps just by chance, the right trend of the data with increasing temperatures, whereby we consider the very slight maximum in Fig. 3 as not relevant in this context. Compare Fig. 3 with the Fig. 5. The latter depicts the results of our fall-off analysis.

Combining k_{rec} with k_{diss} gives

$$K_c(T) = 7.66 \times 10^4 \exp(-6.633 \times 10^4/T + 0.1764 \times 10^8/T^2) \text{ mol cm}^{-3}$$

Now, as one would expect it, the calculated $DH_{r,0}$ values turned out to be closer to each other: 1200 K: $DH_{r,0} = 80.58$ kcal mol^{-1}; 1400 K: $DH_{r,0} = 81.21$ kcal mol^{-1}; 1600 K: $DH_{r,0} = 80.71$ kcal mol^{-1}. The mean value is $DH_{r,0} = 80.83 \pm 0.35$ kcal mol^{-1} (standard deviation). Based upon this enthalpy of reaction, the values $DH_{f,0}$ and $DH_{f,298}$ for cyclopentadienyl were calculated and are given in Table V. It may be noted here that calculating $K_c(T)$ directly from the data given in

Table V Enthalpy of Formation of c-C_5H_5

Reaction: $C_5H_6 \rightarrow$ c-$C_5H_5 + H$; $DH_{r,0} = 80.8 \pm 1$ kcal mol^{-1}

Species	$DH_{f,0}$ (kcal mol^{-1})	$DH_{f,298}$ (kcal mol^{-1})	References
C_5H_6	36.2	32.09^a	[16]
	37.3	33.2^a	[27]
H	51.63	52.10	[16]
c-C_5H_5	65.4 ± 1	62.5 ± 1	Present work /Burcat
	64.3 ± 1	61.4 ± 1	Present work /Roth et al.

Enthalpy of formation at 298 K of c-C_5H_5 from literature

$DH_{f,298}$ (kcal mol^{-1})	Method	References
58 ± 2	Experimental	[28]
61 ± 2	Experimental	[29]
63 ± 2	Experimental	[30]
65.3	Experimental	[11]
63.6	Theoretical	[31]
62–62.6	Theoretical	[12]
62.6	Theoretical	[13]

[a] No standard deviation available.

[14] and applying these to our K_c, $\exp(T)$, resulted in a reaction enthalpy $DH_{r,298} = 82.2$ kcal mol^{-1}. This corresponds to a $DH_{r,0} = 80.5$ kcal mol^{-1}. The differences to the data of Table V are practically negligible.

Fall-Off Analysis

We undertook a simple fall-off analysis by using the interpolation scheme of Troe (see [32a,b]). The interpolation scheme needs as input parameters the rate coefficient for the low pressure limit $k^0_{\text{diss,sc}}$ (sc = strong collision case), the coefficient for the high pressure limit k^∞_{diss}, and the weak collision factor β_c.

Low Pressure Rate Coefficient $\boldsymbol{k^0_{\text{diss,sc}}}$. The low pressure rate coefficient was calculated including rotational effects. The effective dissociation energy $E_0(J)$ depends upon the main quantum number J for rotation. It is assumed (see [33]) that J is conserved while the activated molecule is dissociating.

$$\begin{aligned} E_0(J) &= E_0(0) + B_1[E_{\text{rot,B}}]^p - E_{\text{rot,B}} \\ E_{\text{rot,B}}(J) &= \bar{B}J(J+1) \\ \bar{B} &= \sqrt{AB} \end{aligned} \tag{1}$$

$\bar{B}$ is calculated from the geometric mean of the two similar moments of inertia, A and B, given in Table III. This is sufficient for an almost symmetric oblate top as is the case here. $E_0(0) = DH_{r,0}$ is the exit of a Morse-potential for $J = 0$ associated with the dissociating bond C—H. The Morse potential for the H-atom fission was modeled as

$$V_M(\Delta r) = D_M(1 - \exp(-\Delta r/\beta_M))^2$$

D_M is connected to $DH_{r,0}$ by

$$D_M = DH_{r,0} + E_z(C_5H_6) - E_z(\text{c-}C_5H_5) \tag{2}$$

$E_z(i)$ is the zero-point energy of the molecule i.

β_M is the scaling factor for the Morse potential and is connected to D_M and the force constant pertinent to the vibration of the breaking C—H bond.

$$\beta_M = \sqrt{2D_M/k_{v,\text{RC}}}$$

In our case $k_{v,\text{RC}} = 4.8 \times 10^5$ dyne cm^{-1} (see [34]). The C_5H_6 molecule was considered as a symmetric top.

The effective potential V_{eff} for the dissociating C—H bond for $J > 0$ can be approximately modeled as (see [35]):

$$\begin{aligned} V_{\text{eff}}(J, \Delta r) \approx{}& V_M(\Delta r) + E_{\text{rot,B}}(J)\frac{I(\Delta r = 0)}{I(\Delta r)} \\ &+ (E_{z,0} - E_{z,p})\exp(-\Delta r/\alpha_{\text{Troe}}) + E_{z,p} \end{aligned} \tag{3}$$

$I(\Delta r)$ is the mean of the two smaller moments of inertia of cyclopentadiene changing with the lengthening of the dissociating C—H bond

$$\begin{aligned} E_{\text{rot,B}}(J) &= \bar{B}J(J+1) \\ E_{z,0} &= E_z(C_5H_6) - \frac{v_{\text{RC}}}{2} \end{aligned}$$

v_{RC} is the frequency of one of the C—H stretch vibrations of the CH_2 group. RC denotes the reaction coordinate; $E_{z,p}$ is the zero-point energy of cyclopentadienyl ($E_{z,\text{c-}C_5H_5}$). The last two terms in Eq. (3) approximately take into account that with increasing C—H distance the two C—H bending vibrations of the CH_2 group (scissors and twist) eventually go over into rotations of the cyclopentadienyl radical. α_{Troe} is a scaling parameter that was found empirically to be in the order of 1 Å by Quack and Troe [36]. The parameters B_1 and p were simply calculated by assuming that during the lengthening of one of the C—H bonds in the CH_2-group, neither the bond angle nor the structure of the c-C_5H_5-rest does change.

With these assumptions we calculated the moments of inertia dependent on the distance C—H. The effective potential $V_{\mathrm{eff}}(J, \Delta r)$ exhibits maxima at varying distances. These maxima were determined and the associated effective dissociation energy $E_0(J)$ was modeled accordingly to Eq. (1). The parameters are $B_1 = 0.763$ (kcal mol^{-1})$^{1-p}$ and $p = 1.02$.

We modeled the total rotational energy for the dissociating cyclopentadiene molecule as $E_{\mathrm{rot}}(J) \approx \bar{B}J(J+1) + (C - \bar{B})K^2$. Since $C < \bar{B}$, the last term is always negative. The rotational states, associated with the largest moment of inertia, were convoluted into the vibrational density of states, $\rho_{v,K}(E)$, following a proposal of Troe [32c]. The reason for doing so is that due to rotation–vibration interaction the K-states may not stay stable, while J is assumed to be conserved during the dissociation of the activated molecule.

The densities of states $\rho_{v,K}(E)$ were directly calculated with an energy step size of 20 cm^{-1}. The $|K| \leq J$ restriction was regarded. Our calculations were based upon harmonic vibrations. The frequencies of the cyclopentadiene were taken from Castelucci et al. [24].

$k^0_{\mathrm{diss,sc}}$[cm^3 mol^{-1} s^{-1}] was obtained from a somewhat simplified model:

$$k^0_{\mathrm{diss,sc}} = Z_{\mathrm{LJ}} RT \sum_{J=0}^{J=J_{\mathrm{end}}} \times \frac{(2J+1)\exp(-\bar{B}J(J+1)/RT)}{Q_{\mathrm{C_5H_6}}} \times F(E_0(J))\rho_{v,K}(E_0(J))\exp(-E_0(J)/RT) \tag{4}$$

J_{end} is a suitably chosen number large enough to assure that in the given experimental T-range $k^0_{\mathrm{diss,sc}}$ practically does not depend on J for $J > J_{\mathrm{end}}$. The factor $F(E_0(J))$ is defined [33] as:

$$F(E_0(J)) = \frac{1}{RT} \int_{E=E_0(J)}^{\infty} f_v(E)/f_v(E_0(J))\,\mathrm{d}E.$$

$f_v(E)$ is the Boltzmann distribution function for vibration energies between E and $E + \mathrm{d}E$. For the Lennard–Jones collisions frequency Z_{LJ} [cm^3 mol^{-1} s^{-1}], the collision parameters determining Z_{LJ}, σ_i, and $(\varepsilon/k)_i (i = \mathrm{AR, KR, C_5H_6})$ were calculated from the semiempirical formulae given by Cambi et al. [37] (see Table III).

The rate coefficient at the low pressure limit including weak collision effects is defined as $k^0_{\mathrm{diss,wc}} = \beta_c k^0_{\mathrm{diss,sc}}$. The weak collision coefficient β_c is approximately connected to $-\langle \Delta E \rangle^{(0)}_{\mathrm{all}}$ as outlined in [32d]:

$$\frac{\beta_c}{1 - \beta_c^{1/2}} \approx \frac{-\langle \Delta E \rangle^{(0)}_{\mathrm{all}}}{F(E_0)RT} \quad F(E_0) \leq 3 \tag{5}$$

Equation (5) was derived assuming a simple exponential model for the energy transfer between the bath gas molecules and the dissociating molecule. The probability of the “down” process (energy transfer to the bath gas) is modeled as [32d]

$$P^{(\mathrm{down})}_{i,j} = K(E_i)\,e^{-(E_i - E_j)/\alpha} \quad \text{for} \quad E_j \leq E_i$$

α is an empirical model depending parameter that has to be extracted from comparisons between experiments and a theoretical model. Generally, for any energy transfer model the two Eqs. (6) and (7), define $\langle \Delta E \rangle_{\mathrm{all}}$:

$$1 = \int_{E_j=0}^{\infty} P(E_j, E_i)\,\mathrm{d}E_j \quad \text{for any given } E_i \tag{6}$$

In particular, $\langle \Delta E \rangle_{\mathrm{all}}$ is defined for $E_i = E_0$ as

$$\langle \Delta E \rangle_{\mathrm{all}} = \int_{E_j=0}^{\infty} (E_j - E_0) P(E_j, E_0)\,\mathrm{d}E_j \tag{7}$$

By an approximate integration of Eqs. (6) and (7) in the frame of the exponential energy transfer model it is shown that

$$\langle \Delta E \rangle_{\mathrm{all}} \approx -\frac{\alpha^2}{\alpha + F(E_0)RT} \equiv \langle \Delta E \rangle^{(0)}_{\mathrm{all}} \tag{8}$$

if $F(E_0) < 3$ [32d].

Modelling of experimental data exhibits that either for a RRKM interpolation or the more sophisticated interpolation scheme of Gilbert et al. [32b], $\langle \Delta E \rangle_{\mathrm{all}} \approx \langle \Delta E \rangle^{(0)}_{\mathrm{all}}$ can be assumed to stay approximately constant over a rather large temperature range ([38]; see also the recent review contained in [39]). For example, for the $\mathrm{CH_4}$-dissociation, Cobos and Troe [40] could model experimental data sufficiently well with a practically constant $\langle \Delta E \rangle^{(0)}_{\mathrm{all}}$ and the associated β_cs [Eq. (5)] over a temperature range from 1000 to 5000 K. In the $\mathrm{CH_4}$ case the values for $F(E_0)$ are for all temperatures <3. $\langle \Delta E \rangle_{\mathrm{all}}$ depends on the nature of the collision partner. In many experimental studies on reaction kinetics highly diluted mixtures of the investigated molecule with noble gases were used. This simplifies the data reduction, since the energy transfer to and from the molecule is in this case practically determined by the diluent.

Unfortunately, the use of Eq. (5) is for larger molecules restricted to not too high temperatures. Equation (5) becomes increasingly inaccurate if the temperature dependent $F(E_0)$ exceeds a limit of about 3 (see [32b]).

For the T-range of our experiments $F(E_0) \leq 3$ is fulfilled; however, for the T-range of the experiments of Kern et al. [11] this is not true for all data. For their applied experimental conditions an improved expression for β_c has to be used [see [32b], Eq. (4.7)]. We assumed that $\langle \Delta E \rangle_{\mathrm{all}}^{(0)}$ stays constant for $F(E_0) < 3$ for both experimental sets. But for $T > 1600$ K, $F(E_0)$ increasingly exceeds to 3 and so we had to empirically find data for α such that the experimental rate coefficients of Kern et al. for $T > 1600$ K can be simulated. We calculated α from Eq. (8) for an assumed constant $\langle \Delta E \rangle_{\mathrm{all}}^{(0)}$ for $T \leq 1600$ K. For larger temperatures the parameters α were fitted to the experimental rate coefficients using Eqs. (6) and (7). The obtained $\alpha(T)$ were inserted in the improved relation for β_c as given in [32b]:

$$\beta_{\mathrm{c}} = \left(\frac{\alpha}{\alpha + F(E_0)RT} \right)^2 \times \frac{1}{\int_0^{E_0} f_v(E) \left[1 - \frac{F(E_0)\,RT}{\alpha + F(E_0)\,RT} \; \exp(-(E_0 - E)/F(E_0)RT) \right] \mathrm{d}E}$$

For further details the reader should refer to the work of Gilbert et al. [32b].

High Pressure Rate Coefficient $k_{\mathrm{diss}}^{\infty}$. We modeled the needed high pressure rate coefficient by

$$k_{\mathrm{diss}}^{\infty} = k_{\mathrm{rec}}^{\infty}\, K_{\mathrm{c}}(T)$$

Since it is expected that $k_{\mathrm{rec}}^{\infty}$ does not strongly vary with temperature for simple bond fissions, we have set, in a probably good approximation, $k_{\mathrm{rec}}^{\infty} =$ constant over the temperature range of our measurements. Appropriate examples to support this assumption are reviewed in Baulch et al. ([41], Table III] .

Modeling of Measured Data. The formalism of Troe [32a] and of Gilbert et al. [32b] was applied to the dissociation of cyclopentadiene:

$$\begin{aligned} \frac{k_{\mathrm{diss}}(M)}{k_{\mathrm{diss}}^{\infty}} &= \left(\frac{k_{\mathrm{diss,wc}}^{0}\; M/k_{\mathrm{diss}}^{\infty}}{1 + k_{\mathrm{diss,wc}}^{0}\; M/k_{\mathrm{diss}}^{\infty}} \right) \\ &\quad \times F_{\mathrm{sc}}\big(k_{\mathrm{diss,wc}}^{0}\; M/k_{\mathrm{diss}}^{\infty}\big) \\ &\quad \times F_{\mathrm{wc}}\big(k_{\mathrm{diss,wc}}^{0}\; M/k_{\mathrm{diss}}^{\infty}\big) \qquad (9) \end{aligned}$$

The factor F_{wc} contains effects associated with the energy transfer by collisions of the molecule with the bath gas; F_{wc} is a function of β_c EMBED.

Troe [32(a), (d)] derived the interpolation scheme by neglecting effects of external rotation. We assumed that it should work as well, if we insert for $k_{\mathrm{diss,sc}}^{0}$ the full expression of Eq. (4). Two parameters were varied: $k_{\mathrm{rec}}^{\infty}$ $\langle \Delta E \rangle_{\mathrm{all}}^{(0)}[\mathrm{cm}^{-1}]$ and (the average energy transferred by collision). The needed $k_{\mathrm{diss}}^{\infty}$ in Eq. (9) was provided by

$$k_{\mathrm{diss}}^{\infty} = k_{\mathrm{rec}}^{\infty} K_{\mathrm{c}}(T)$$

We arrived at a good representation of our measured data with a variety of pairs of $k_{\mathrm{rec}}^{\infty}$ and $-\langle \Delta E \rangle_{\mathrm{all}}^{(0)}$ (see Figs. 4 and 5).
T ≤ 1600 K:

$$\begin{aligned} k_{\mathrm{rec}}^{\infty} &= 3.5 \times 10^{14}\ \mathrm{cm}^3\ \mathrm{mol}^{-1}\ \mathrm{s}^{-1}\ \text{ and} \\ &\quad -\langle \Delta E \rangle_{\mathrm{all}}^{(0)} = 130\ \mathrm{cm}^{-1} \\ &\qquad \text{(not given in the figures)} \\ k_{\mathrm{rec}}^{\infty} &= 4.2 \times 10^{14}\ \mathrm{cm}^3\ \mathrm{mol}^{-1}\ \mathrm{s}^{-1}\ \text{ and} \\ &\quad -\langle \Delta E \rangle_{\mathrm{all}}^{(0)}\ \text{EMBED} = 75\mathrm{cm}^{-1} \\ k_{\mathrm{rec}}^{\infty} &= 5.0 \times 10^{14}\ \mathrm{cm}^3\ \mathrm{mol}^{-1}\ \mathrm{s}^{-1}\ \text{ and} \\ &\quad -\langle \Delta E \rangle_{\mathrm{all}}^{(0)}\ \text{EMBED} = 25\mathrm{cm}^{-1} \end{aligned}$$

The reason for this arbitrariness is simply the low sensitivity of our experiments on the low pressure rate coefficient, since our experiments were performed rather close to the high pressure limit.

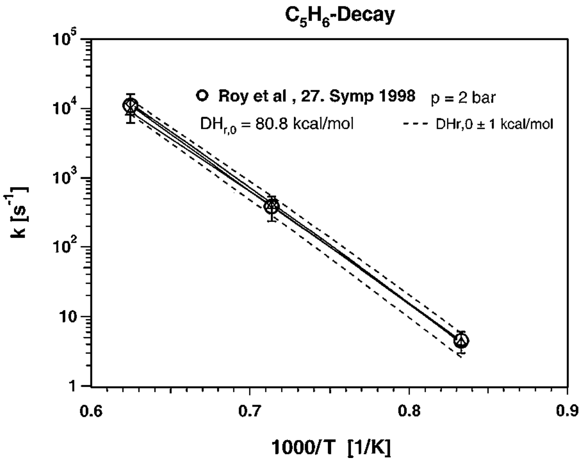

Figure 4 Results of the fall-off analysis for $k_{\mathrm{diss}}(M)$. Experimental data from Roy et al. [7] (see text); $\diamondsuit - \langle \Delta E \rangle_{\mathrm{all}}^{(0)} = 75\ \mathrm{cm}^{-1}; k_{\mathrm{rec}}^{\infty} = 4.2 \times 10^{14}\ \mathrm{cm}^3\ \mathrm{mol}^{-1}\ \mathrm{s}^{-1}$; $\Delta - \langle \Delta E \rangle_{\mathrm{all}}^{(0)} = 25\ \mathrm{cm}^{-1}; k_{\mathrm{rec}}^{\infty} = 5.0 \times 10^{14}\ \mathrm{cm}^3\ \mathrm{mol}^{-1}\ \mathrm{s}^{-1}$.

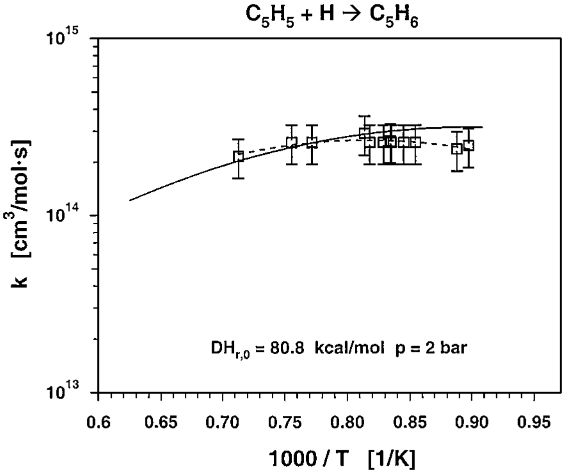

Figure 5 Results of the fall-off analysis for $k_{\mathrm{rec}}(M)$ (see text); broken line: regression from Fig. 3; solid line: $-\langle \Delta E \rangle_{\mathrm{all}}^{(0)} = 25\ \mathrm{cm}^{-1}$; $k_{\mathrm{rec}}^{\infty} = 5.0 \times 10^{14}\ \mathrm{cm}^3\ \mathrm{mol}^{-1}\ \mathrm{s}^{-1}$.

For the temperature range from 1000 to 2500 K we have calculated (Eq. (4))

$$\begin{aligned} k_{\mathrm{diss,sc}}^{0}(\mathrm{AR}) &= 1.07 \times 10^{80}\ T^{-16.788} \\ &\quad \times \exp(-8547.9/T)\ \mathrm{cm}^3\ \mathrm{mol}^{-1}\ \mathrm{s}^{-1} \\ k_{\mathrm{diss,sc}}^{0}(\mathrm{KR}) &= 9.86 \times 10^{79}\ T^{-16.793} \\ &\quad \times \exp(-8543.3/T)\ \mathrm{cm}^3\ \mathrm{mol}^{-1}\ \mathrm{s}^{-1} \\ k_{\mathrm{diss}}^{\infty} &= 7.65 \times 10^{19} \times T^{-1.183} \\ &\quad \times \exp(-42513/T)\ \mathrm{s}^{-1}\ \text{for} \\ k_{\mathrm{rec}}^{\infty} &= 5.0 \times 10^{14}\ \mathrm{cm}^3\ \mathrm{mol}^{-1}\ \mathrm{s}^{-1}. \end{aligned}$$

DISCUSSION

Enthalpy of Formation of the Cyclopentadienyl Radical

The average enthalpy of reaction, $\mathrm{D}H_{\mathrm{r},0}$, extracted from our measured data of $k_{\mathrm{diss}}(T, 2\ \mathrm{bar})$ and $k_{\mathrm{rec}}(T, 2\ \mathrm{bar})$ is 80.8 kcal mol^{-1} for the reaction $C_5H_6 \rightarrow$ c-$C_5H_5 + H$. Systematic errors in k_{diss} as well as on k_{rec} may cancel to some degree, since the main source for these errors is the determination of the absolute concentration of the reactants in the mixture filled in the shock tube. This was considered by our analysis of probes taken from the shock tube. Remaining random errors are ascribed to the measured k_is only. We have assumed that the temperature is accurately given. Consequently, random errors in T appear in the k_i.

We take from the regression analysis the average relative deviation of the measured points from the regression line. If $Y(l)$ is the lth measured value, the associated interpolated number is $Y_{\mathrm{ip}}(l)$. In a very simple approach we may construct the average relative deviation for a set of L measured points:

$$\frac{1}{L}\sum_{l=1}^{L}\sqrt{\frac{(Y(l) - Y_{\mathrm{ip}}(l))^2}{Y_{\mathrm{ip}}^2(l)}}$$

Application of this approach to k_{diss} gives ± 0.28 and to $k_{\mathrm{rec}} \pm 0.035$. The relative average deviation of $K_c(l)$ is equal to or smaller than the sum of both ± 0.31. This translates eventually into $\mathrm{D}H_{\mathrm{r},0} = 80.8 \pm 0.66$ kcal mol^{-1} from our measurements at 1200 K and $\mathrm{D}H_{\mathrm{r},0} = 80.8 \pm 0.88$ kcal mol^{-1} from our measurements at 1600 K. Thus, a conservative guess of the standard deviation would be $\mathrm{D}H_{\mathrm{r},0} = 80.8 \pm 1$ kcal mol^{-1}.

The enthalpy of formation of c-C_5H_5 can be calculated by taking the $\mathrm{D}H_{\mathrm{f},0}$ for cyclopentadiene and H from Table V. We arrive at $\mathrm{D}H_{\mathrm{f},0} = 65.4$ kcal mol^{-1} for c-C_5H_5. This value contains the uncertainty of the $\mathrm{D}H_{\mathrm{f},0}$ of cyclopentadiene. In a recent publication by Roth et al. [27] these authors propose a new value, supported by semiempirical calculations: $\mathrm{D}H_{\mathrm{f},298} = 33.2$ kcal mol^{-1} instead of 32.1 kcal mol^{-1} as given in Burcat's tables [23]. The $\mathrm{D}H_{\mathrm{f},298}$ of c-C_5H_5 would then be reduced to 61.4 kcal mol^{-1} (see Table V).

Modeling of the Fall-Off

Our simulations are based upon the enthalpy of reaction obtained in the present work for $C_5H_6 \rightarrow$ c-$C_5H_5 + H$. The two parameters, $k_{\mathrm{rec}}^{\infty}$ and $\langle \Delta E \rangle_{\mathrm{all}}^{(0)}$, were varied in order to arrive at a satisfying fit of our experimental data. A good fit can be obtained with pairs of $k_{\mathrm{rec}}^{\infty}$ and $\langle \Delta E \rangle_{\mathrm{all}}^{(0)}$, which are bound to a certain range. So we have to accept some arbitrariness. Our experimental conditions were such that the reaction proceeded rather close to the high pressure limit. This is in contrast to the measurements by Kern et al. [11]. In those experiments the reaction was studied closer to the low pressure limit, in particular, if T exceeds 1500 K. Our experiments are more sensitive to the selected value for $k_{\mathrm{rec}}^{\infty}$, whereas Kern's and Kiefer's experiments depend stronger on $\langle \Delta E \rangle_{\mathrm{all}}^{(0)}$. A simple direct comparison of the respective modeling of the two experimental data sets, the present work and that of Kern et al. [11], is not easily possible. The latter group applied a RRKM analysis not taking into account effects of external rotation. Their derived $-\langle \Delta E \rangle_{\mathrm{all}}^{(0)}$ was found on the order of 18 cm^{-1}. For noble gases as main collision partners, numbers for large molecules are reported to lie in the range between 50 and 200 cm^{-1} (see e.g. [38,42]). We tried to find a set of numbers for $k_{\mathrm{rec}}^{\infty}$ and $-\langle \Delta E \rangle_{\mathrm{all}}^{(0)}$, which could be

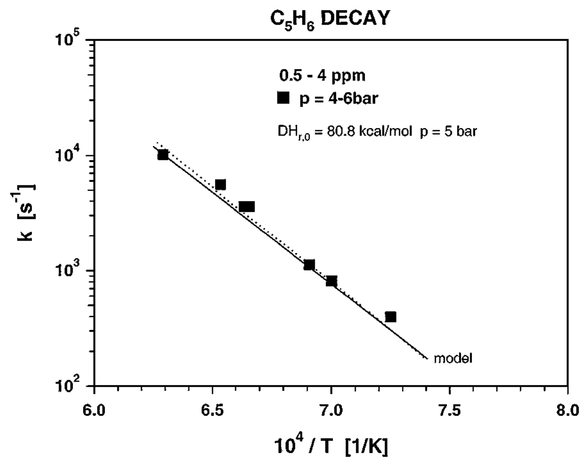

Figure 6 Results of the fall-off analysis for $k_{\text{diss}}(M)$. $p \approx 5$ bar. Calculated with the parameters obtained from the analysis $p = 2$ bar (see text); dotted line: $-\langle \Delta E\rangle_{\text{all}}^{(0)} = 75$ cm^{-1}; $k_{\text{rec}}^{\infty} = 4.2 \times 10^{14}$ cm^3 mol^{-1} s^{-1}; solid line: $-\langle \Delta E\rangle_{\text{all}}^{(0)} = 25$ cm^{-1}; $k_{\text{rec}}^{\infty} = 5.0 \times 10^{14}$ cm^3 mol^{-1} s^{-1}.

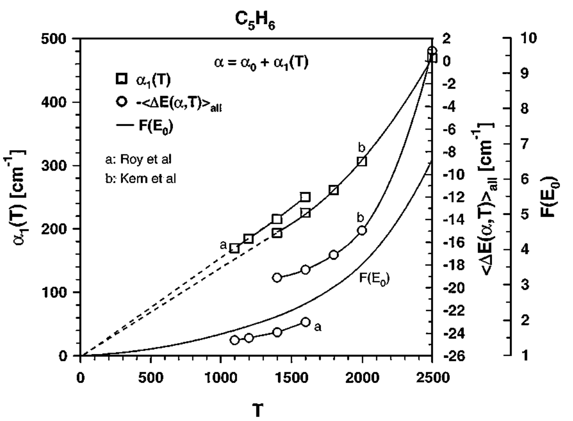

Figure 7 Optimized parameters α for the transition probabilities $P(E_j, E_0)$ (see text). Dotted lines show the extrapolation of $\alpha_1(T)$ to 0. Note the steep increase of $F(E_0)$with T for $T > 1600$ K and note that $-\langle \Delta E\rangle_{\text{all}}$ approaches $-\langle \Delta E\rangle_{\text{all}}^{(0)}$ for low temperatures.

used to reproduce the results of both groups. Starting the simulation of our data with $-\langle \Delta E\rangle_{\text{all}}^{(0)} = 25$ cm^{-1}, which is close to the $-\langle \Delta E\rangle_{\text{all}}^{(0)}$ of Kern et al., led to a satisfying reproduction of our experimental points with a rather high k_{rec}^{∞} of 5.0×10^{14} cm^3 mol^{-1} s^{-1}. However, since we have a barrierless recombination, the value of k_{rec}^{∞}, the "capture rate coefficient," seems plausible. Figure 6 depicts the simulation of our 5 bar experiments. The result is quite acceptable together with $\mathrm{D}H_{\mathrm{r},0} = 80.8$ kcal mol^{-1}.

To reduce the range of optimized parameter pairs as we have extracted them from our experiments, we should have extended our measurements to much lower pressures. Helpful in closing this gap are the data from Kern's and Kiefer's groups.

The simulation of the experiments of Kern et al. [11] cannot be performed with a $-\langle \Delta E\rangle_{\text{all}}^{(0)} = \text{const}$ over their total applied T-range, since for $T > 1600$ K, $F(E_0)$ gets larger than the critical value of about 3. [32b]. The simple relation $\langle \Delta E\rangle_{\text{all}}^{(0)} = -\frac{\alpha^2}{\alpha + F(E_0)RT}$ does not represent $\langle \Delta E\rangle_{\text{all}}$ [Eq. (7)] for high temperatures and large $F(E_0)$. For $T > 1600$ K the simple approximation $\frac{\rho(E)}{\rho(E_0)}\, e^{-(E-E_0)/RT} \approx e^{-(E-E_0)/F(E_0)RT}$ $E \geq E_0$, $J = 0$, as used by Troe [32c] to calculate the $P(E_j, E_0)$ for the c-C$_5$H$_6$ system is inaccurate and therefore not applicable. We calculated the $P(E_j, E_0)$ directly by solving the associated integral equation

$$1 = \int_{E_i=0}^{\infty} P(E_j, E_i)\, \mathrm{d}E_j \quad \text{for } E_i = E_0$$

applying an energy spacing of 10 cm^{-1}. With the obtained $P(E_j, E_0)$, which are functions of the assumed α and of T, the integrals

$$\langle \Delta E\rangle_{\text{all}} = \int_{E_j=0}^{\infty} (E_j - E_0)\, P(E_j, E_0)\, \mathrm{d}E_j$$

were calculated.

We fitted empirically the experimental results of Kern et al. with α by $\alpha = \alpha_0 + \alpha_1(T)$. Figure 7 depicts the results. (Note: for low temperatures $-\langle \Delta E\rangle_{\text{all}}^{(0)}$ approaches α EMBED, therefore, $\alpha_1(T) \rightarrow 0$ for $T \rightarrow 0$; $-\langle \Delta E\rangle_{\text{all}}^{(0)}$ as well as $-\langle \Delta E\rangle_{\text{all}}$ are then practically determined by α alone since $F(E_0) \rightarrow 1$ at low temperatures and consequently $-\langle \Delta E\rangle_{\text{all}}^{(0)} \rightarrow -\langle \Delta E\rangle_{\text{all}}$. It clearly turns out that for low temperatures the calculated $-\langle \Delta E\rangle_{\text{all}}$ approaches $-\langle \Delta E\rangle_{\text{all}}^{(0)}$, but for higher temperatures $-\langle \Delta E\rangle_{\text{all}}$ contains increasing contributions from the energy flux from the bath gas into the cyclopentadiene molecule with increasing temperature.

The needed β_{c}s were calculated for given αs by solving the master equation for the c-C$_5$H$_5$ system (M $\rightarrow$ 0). It was verified that indeed the simplified formula for β_{c}, as given above, resulted in β_{c} values within about 10% of the data from the solution of the master equation. This was already observed by Gilbert et al. [32b]. Our simulation with $k_{\text{rec}}^{\infty} = 5.0 \times 10^{14}$ cm^3 mol^{-1} s^{-1} of Kern's and Kiefer's experimental results is shown in Fig. 8. The lines in Fig. 8, which were taken from [11], represent the RRKM interpolation for 0.6 and 0.266 bar. Kern et al. [11] give $k(M)$ in units of cm^3 mol^{-1} s^{-1}. We have converted their data by multiplying them

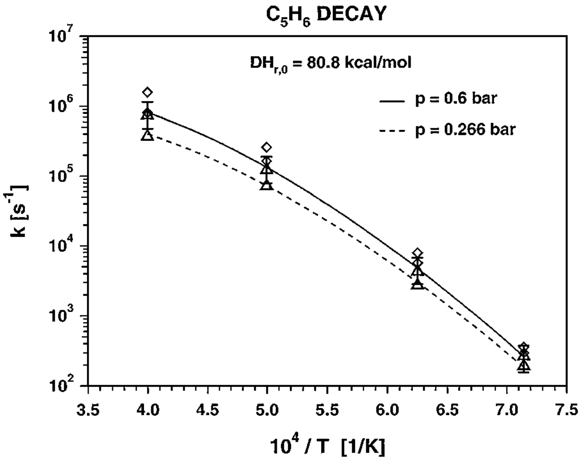

Figure 8 Dissociation of C_5H_6 at low pressures. Data taken from [11]. The symbols represent results from our fall-off analysis applied to the experimental conditions of [11] (see text). $\diamond - \langle \Delta E \rangle^{(0)}_{\text{all}} = 75\ \text{cm}^{-1}; k^{\infty}_{\text{rec}} = 4.2 \times 10^{14}$ cm^3 mol^{-1} s^{-1} $\alpha(T)$ from Eq. (8) for the whole T-range. $\Delta - \langle \Delta E \rangle^{(0)}_{\text{all}} = 20\ \text{cm}^{-1}; k^{\infty}_{\text{rec}} = 5.0 \times 10^{14}$ cm^3 mol^{-1} s^{-1} $\alpha(T)$ for $T > 1600$ K fitted to experimental data.

with M to obtain the ks in units of s^{-1}. The error bars are guessed from their Fig. 2 in [11]. Since the experimental conditions applied by Kern et al. allow measurements closer to the low pressure limit, the sensitivity on k^{∞}_{rec} of our modeling is rather low. A satisfying modeling of Kern's data with the pair $k^{\infty}_{\text{rec}} = 4.2 \times 10^{14}$ cm^3 mol^{-1} s^{-1} and $-\langle \Delta E \rangle^{(0)}_{\text{all}} = 75$ cm^{-1} for the whole experimental T-range is not possible. One observes even for $T \leq 1600$ K a rather bad fit of the experimental data. Presently, we propose the optimized sets: $k^{\infty}_{\text{rec}} = 5.0 \times 10^{14}$ cm^3 mol^{-1} s^{-1} and $-\langle \Delta E \rangle^{(0)}_{\text{all}}$ between 20 and 25 cm^{-1} (for $T \leq 1600$ K) by which the experiments given in [11] can be sufficiently well modeled. $\alpha(T)$ for $T \leq 1600$ K was taken from Eq. (8). For higher temperatures $\alpha(T)$ was fitted to the experimental data. In Fig. 8, we show the modeling for $-\langle \Delta E \rangle^{(0)}_{\text{all}} = 20$ cm^{-1}.

CONCLUSIONS

Our direct measurements of the forward and backward reaction coefficients for $C_5H_6 \rightleftharpoons c\text{-}C_5H_5 + H$ led us to an enthalpy of reaction $DH_{r,0} = 80.8 \pm 1$ kcal mol^{-1} for the reaction $C_5H_6 \rightarrow c\text{-}C_5H_5 + H$ and to enthalpies of formation for cyclopentadienyl of $DH_{f,0} = 65.4 \pm 1$ kcal mol^{-1} and $DH_{f,298} = 62.5 \pm 1$ kcal mol^{-1}, respectively. The latter value is somewhat smaller than a recent number $DH_{f,298} = 65.3 \pm 2$ kcal mol^{-1} obtained by Kern et al. [11], based upon their RRKM modeling of the cyclopentadiene decay measured at low pressures ranging from 100 to 450 Torr. However, our result compares favorably with recently theoretically obtained numbers by Wang and Brezinsky [12] and by Moskaleva and Lin [13] as well as with older experimental data from Bartmess et al. [29] and DeFrees et al. [29]. The determination of the enthalpy of formation of cyclopentadienyl was made possible only by taking the quite recently calculated entropy data for cyclopentadienyl from Kiefer et al. [14]. Attempts to model the entropy of c-C_5H_5 by inadequate assumptions concerning the contribution of the facile valence isomerization to the entropy ([12,13]) lead to a formation enthalpy of the cyclopentadienyl radical considerably off the numbers presented here.

The fall-off analysis performed depends strongly on accurately calculated data for $K_c(T)$. With these new data satisfying simulations of the dissociation as well as the recombination coefficients in the investigated ranges of pressures and temperatures became possible.

We are greatly indebted to A. Wagner and J. Kiefer for sending us prior to publication their paper on the effect of the Jahn–Teller distortion on the thermodynamic functions of the cyclopentadienyl radical. We also acknowledge stimulating discussions with J. Troe and Hai Wang.

BIBLIOGRAPHY

1. Frank, P.; Herzler, J.; Just, Th.; Wahl, C. Proc Combust Inst 1994, 25, 833–840.
2. Horn, Ch.; Roy, K.; Frank, P.; Just, Th. Proc Combust Inst 1998, 27, 321–328.
3. Melius, C. F.; Colvin, E. C.; Marinov, N. M.; Pitz, W. J.; Senkan, S. M. Proc Combust Inst 1996, 26, 685–692.
4. Bittner, J. D.; Howard, J. B. Proc Combust Inst 1980, 18, 1105.
5. Lindstedt, R. P.; Skevis, G. Combust Flame 1994, 99, 551–561 .
6. Bittker, D. A. Combust Sci Tech 1991, 79, 49–72.
7. Roy, K.; Horn, Ch.; Frank, P.; Slutsky, V. G.; Just, Th. Proc Combust Inst 1998, 27, 329–336.
8. (a) Dean, A. M. J Phys Chem 1990, 94, 1432–1439; (b) Zhong, X.; Bozzelli, J. W. J Phys Chem A 1998, 102, 3537–3555.
9. Emdee, J. L.; Brezinsky, K.; Glassman, I. J Phys Chem 1992, 96, 2151–2161.
10. Lovell, A. B.; Brezinsky, K.; Glassman, I. Proc Combust Inst 1989, 22, 1063–1074.
11. Kern, R. D.; Zhang, Q.; Yao, J.; Jursic, R. S.; Tranter, R. S.; Greybill, M. A.; Kiefer, J. H. Proc Combust Inst 1998, 27, 143–150.
12. Wang, H.; Brezinsky, K. J Phys Chem A 1998, 102, 1530–1541.

13. Moskaleva, L. V.; Lin, M. C. J Comput Chem 2000, 21, 415–425.
14. Kiefer, J. H.; Tranter, R. S.; Wang, H.; Wagner, A. F. J Phys Chem (in press).
15. Frank, P.; Just, Th. Ber Bunsenges Phys Chem 1985, 89, 181–187.
16. Herzler, J. PhD thesis, DLR, Stuttgart, 1994.
17. Bacskay, G. B.; Mackie, J. C. Phys Chem Chem Phys 2001, 3, 2467–2473.
18. Roy, K.; Frank, P.; Just, Th. To be published.
19. Wintergerst, K. PhD thesis, DLR, Stuttgart, 1993.
20. Roy, K.; Frank, P. Twenty-First International Symposium on Shock Waves and Shock Tubes, 1997.
21. Marinov, N. M.; Pitz, W. J.; Westbrook, C. K.; Castaldi, M. J.; Senkan, S. M. Combust Sci Tech 1996, 116–117, 211–287.
22. Roy, K. PhD thesis, DLR, Stuttgart, 1999.
23. Burcat, A. Third Millenium Ideal Gas and Condensed Phase Thermochemical Database for Combustion Technion-Israel Institute of Technology, TAE 867, January 2001.
24. Castelucci, E.; Manzelli, B.; Fortunato, B.; Gallinella, E.; Mirone, P. Spectrochim Acta A 1975, 31, 451.
25. (a) Meyer, R.; Graf, F.; Ha, Tae-Kyu.; Günthard, Hs. H. Chem Phys Lett 1979, 66, 65–71; (b) Ha, Tae-Kyu.; Meyer, R.; Günthard, Hs. H. Chem Phys Lett 1980, 69, 510–513.
26. Jahn, H. A.; Teller, E. Proc Roy Soc A 1931, 161, 220.
27. Roth, W. R.; Adamczak, O.; Breuckmann, R.; Lennartz, H. W.; Boese, R. Chem Ber 1991, 124, 2499–2521.
28. McMillen, D. F.; Golden, D. M. Ann Rev Phys Chem 1982, 33, 493–532.
29. Bartmess, J. E.; Scott, J. A.; McIver, R. T. J Am Chem Soc 1979, 101, 6046.
30. DeFrees, D. J.; McIver, R. T.; Hehre, W. J. J Am Chem Soc 1980, 102, 3334.
31. Karni, M.; Oref, I.; Burcat, A. J Phys Chem Ref Data 1991, 20, 665.
32. (a) Troe, J. Ber Bunsenges Phys Chem 1983, 87, 161–169; (b) Gilbert, R. G.; Luther, K.; Troe, J. Ber Bunsenges Phys Chem 1983, 87, 169–177; (c) Troe, J. J Chem Phys 1977, 66, 4758–4775; (d) Troe, J. J Chem Phys 1977, 66, 4745–4757.
33. Troe, J. J Phys Chem 1979, 83, 114–126.
34. Herzberg, G. Molecular Spectra and Molecular Structure, Infrared and Raman Spectra of Polyatomic Molecules, van Nostrand, Princeton NJ, 1945.
35. Troe, J. J Chem Phys 1981, 75, 226–237.
36. Quack, M.; Troe, J. Ber Bunsenges Phys Chem 1974, 78, 240–252.
37. Cambi, R.; Cappaletti, D.; Liuti, G.; Pirani, F. J Chem Phys 1991, 95, 1852–1861.
38. Heymann, H.; Hippler, H.; Troe, J. J Chem Phys 1984, 80, 1853–1860.
39. Holbrook, K. A.; Pilling, M. J.; Robertson, S. H. Unimolecular Reactions, 2nd ed. Wiley, New York, 1996, Ch. 9.
40. Cobos, C. J.; Troe, J. Z Phys Chem Neue Folge 1992, 176, 161–171.
41. Baulch, D. L.; Cobos, C. J.; Cox, R. A.; Frank, P.; Hayman, G.; Just, Th.; Kerr, J. A.; Murrells, T.; Pilling, M. J.; Troe, J.; Walker, R. W.; Warnatz, J. J Phys Chem Ref Data 1994, 23, 847–1031.
42. Börjesson, L. E. B.; Nordholm, S. J Phys Chem 1995, 99, 938–944.